THE JOURNAL OF BIOLOGICAL CHEMISTRY VOL. 284, NO. 17, pp. 11134–11141, April 24, 2009

Disulfide Bond Formation Significantly Accelerates the Assembly of Ure2p Fibrils because of the Proximity of a Potential Amyloid Stretch*[S]

Received for publication, December 23, 2008, and in revised form, February 27, 2009 Published, JBC Papers in Press, March 3, 2009, DOI 10.1074/jbc.M809673200

Li Fei[‡§] **and Sarah Perrett**[‡1]

From the [‡]*National Laboratory of Biomacromolecules, Institute of Biophysics, Chinese Academy of Sciences, 15 Datun Road, Chaoyang District, Beijing 100101, China and the* [§]*Graduate University of the Chinese Academy of Sciences, 19 Yuquan Road, Shijingshan District, Beijing 100049, China*

Aggregation of the Ure2 protein is at the origin of the [*URE3*] prion trait in the yeast *Saccharomyces cerevisiae*. The N-terminal region of Ure2p is necessary and sufficient to induce the [*URE3*] phenotype *in vivo* and to polymerize into amyloid-like fibrils *in vitro*. However, as the N-terminal region is poorly ordered in the native state, making it difficult to detect structural changes in this region by spectroscopic methods, detailed information about the fibril assembly process is therefore lacking. Short fibril-forming peptide regions (4–7 residues) have been identified in a number of prion and other amyloid-related proteins, but such short regions have not yet been identified in Ure2p. In this study, we identify a unique cysteine mutant (R17C) that can greatly accelerate the fibril assembly kinetics of Ure2p under oxidizing conditions. We found that the segment QVNI, corresponding to residues 18–21 in Ure2p, plays a critical role in the fast assembly properties of R17C, suggesting that this segment represents a potential amyloid-forming region. A series of peptides containing the QVNI segment were found to form fibrils *in vitro*. Furthermore, the peptide fibrils could seed fibril formation for wild-type Ure2p. Preceding the QVNI segment with a cysteine or a hydrophobic residue, instead of a charged residue, caused the rate of assembly into fibrils to increase greatly for both peptides and full-length Ure2p. Our results indicate that the potential amyloid stretch and its preceding residue can modulate the fibril assembly of Ure2p to control the initiation of prion formation.

The [*URE3*] phenotype of *Saccharomyces cerevisiae* arises because of conversion of the Ure2 protein to an aggregated propagatable prion state (1, 2). Ure2p contains two regions: a poorly structured N-terminal region and a compactly folded C-terminal region (3, 4). The N-terminal region is rich in Asn and Gln residues, is highly flexible, and is without any detectable ordered secondary structure (4–6). This region is necessary and sufficient for prion behavior *in vivo* (2) and amyloid-forming capacity *in vitro* (5, 7), so it is referred to as the prion domain (PrD).[2] The C-terminal region has a fold similar to the glutathione *S*-transferase superfamily (8, 9) and possesses glutathione-dependent peroxidase activity (10). Upon fibril formation, the N-terminal region undergoes a significant conformational change from an unfolded to a thermally resistant conformation (11), whereas the glutathione *S*-transferase-like C-terminal domain retains its enzymatic activity, suggesting that little conformational change occurs (10, 12). Ure2p fibrils show various morphologies, including variations in thickness and the presence or absence of a periodic twist (13–16). The overall structure of the fibrils imaged by cryoelectron microscopy suggests that the intact fibrils contain a 4-nm amyloid filament backbone surrounded by C-terminal globular domains (17).

It is widely accepted that disulfide bonds play a critical role in maintaining protein stability (18–21) and also affect the process of protein folding by influencing the folding pathway (22–25). A recent study shows that the presence of a disulfide bond in a protein can markedly accelerate the folding process (26). Therefore, a disulfide bond is a useful tool to study protein folding. In the study of prion and other amyloid-related proteins, cysteine scanning has been widely used to study the structure of amyloid fibrils, the driving force of amyloid formation, and the plasticity of amyloid fibrils (13, 27–31).

Short segments from amyloid-related proteins, including IAPP (islet amyloid polypeptide), β_2-microglobulin, insulin, and the amyloid-β peptide, show amyloid-forming capacity (32–34). Hence, the amyloid stretch hypothesis has been proposed, which suggests that a short amino acid stretch bearing a highly amyloidogenic motif might supply most of the driving force needed to trigger the self-catalytic assembly process of a protein to form fibrils (35, 36). In support of this hypothesis, it was found that the insertion of an amyloidogenic stretch into a non-amyloid-related protein can trigger the amyloidosis of the protein (36). At the same time, the structural information obtained from microcrystals formed by amyloidogenic stretches and bearing cross-β-structure has contributed significantly to our understanding of the structure of intact fibrils at the atomic level (34, 37). However, no amyloidogenic stretches <10 amino acids have so far been identified in the yeast prion protein Ure2.

* This work was supported by National Natural Science Foundation of China Grants 30470363, 30620130109, 30670428, and 30870482; Chinese Ministry of Science and Technology Grants 2006CB500703 and 2006CB910903; and Chinese Academy of Sciences Knowledge Innovation Project KSCX2-YW-R-119.

[S] The on-line version of this article (available at http://www.jbc.org) contains supplemental Figs. S1–S6.

[1] To whom correspondence should be addressed. Tel.: 86-10-6485-6727; Fax: 86-10-6487-2026; E-mail: sarah.perrett@iname.com.

[2] The abbreviations used are: PrD, prion domain; ThT, thioflavin T; DTT, 1,4-dithiothreitol; WT, wild-type; EM, electron microscopy.

In this study, we performed a cysteine scan within the N-terminal PrD of Ure2p and found a unique cysteine mutant (R17C) that eliminates the lag phase of the Ure2p fibril assembly reaction upon the addition of oxidizing agents. Furthermore, we identified a 4-residue region adjacent to Arg^{17} as a potential amyloid stretch in Ure2p.

EXPERIMENTAL PROCEDURES

Materials—Tris, NaCl, thioflavin T (ThT), and cumene hydroperoxide were from Sigma, and 1,4-dithiothreitol (DTT) was from Merck. All other reagents were local products of analytical grade. Lyophilized synthetic peptides were purchased from Scilight Biotechnology (Beijing, China). The peptides were supplied as the trifluoroacetate salt, and the purity (>98%) and composition were confirmed by high performance liquid chromatography and electrospray mass spectroscopy. Peptide solutions were prepared by weighing the amount of peptide and dissolving in Buffer A (50 mM Tris (pH 8.4) and 200 mM NaCl). The peptide concentration was confirmed by the BCA assay (Pierce).

Protein Preparation—All mutants of Ure2p were obtained by PCR using a synthetic wild-type (WT) *URE2* gene as a template (4) and confirmed by DNA sequencing of the entire gene. WT Ure2p and all mutational variants were produced in *Escherichia coli* with a short His tag using the expression vector mini-pRSETa as described (4). *E. coli* C41 cells (38) harboring the WT or mutant *URE2* plasmid were grown at 37 °C in 2YT medium supplemented with 100 μg/ml ampicillin with vigorous shaking until they reached an absorbance of 0.6 at 600 nm. Protein expression was induced for 10 h at 16 °C using 0.2 mM isopropyl β-D-thiogalactopyranoside. Cell lysis was performed using a French press, and subsequent protein purification was performed under native conditions as described previously (4).

Protein purity was checked by SDS-PAGE, and the protein concentration was determined from the absorbance at 280 nm on a Shimadzu UV-2501 instrument using a molar extinction coefficient of 48,220 M^{-1} cm^{-1} (4). R17F, R17L, and R17C and its truncated variants were purified immediately before use; buffer exchange was performed rapidly using a desalting column (HiTrap desalting, GE Healthcare), and the proteins were then used directly for experiments because of their tendency to form fibrils extremely rapidly, even during the processes of freezing and thawing. Other proteins were prepared in an identical manner and used immediately or were dialyzed at 4 °C, flash-frozen, and stored at −80 °C in Buffer A; the latter leads to slightly faster fibril formation presumably because of the presence of small quantities of preformed seeds (15, 39). Therefore, for direct comparison of mutants (*i.e.* data shown in a single figure panel), the process of purification, preparation, and incubation of proteins was always performed in an identical manner in parallel.

Amyloid Fibril Formation—The kinetics of amyloid formation of Ure2p and its variants were monitored using ThT binding fluorescence as described previously (14). Incubation was at a constant temperature of 8 °C without shaking. At regular time intervals, 10-μl aliquots were withdrawn from the reaction mixture and assayed for ThT binding. ThT binding was measured by averaging the emission signal over 10 s using a Hitachi F4500 spectrofluorometer set at 450 nm (excitation) and 485 nm (emission), with slit widths of 5 nm. The assembly of peptides into fibrils was performed at 8 °C at concentrations ranging from 1 to 4 mg/ml. The peptide CQVNIGNR was incubated without agitation. For all other peptides, agitation (1000 rpm; MS_2 minishaker, IKA) was used to shorten the lag time.

Fibril and Seed Preparation—Amyloid fibrils made from Ure2p and its mutants or peptides were collected by centrifugation (18,000 × *g*, 30 min), washed twice with Buffer A, and resuspended in Buffer A. Seeds of fibrils were prepared by sonicating preformed fibrils for 1 min at 30% amplitude using a Vibra-Cell sonicator (Sonics & Materials, Inc.).

To determine the protein concentration of the fibril preparation, an aliquot of the resuspended fibrils was removed; 2% SDS was added; and the solution was boiled for 5 min, upon which the cloudy resuspension became transparent. The protein concentration was then determined by UV absorption or BCA assay.

Assay of enzymatic activity of fibrils was performed as described (10). Proteinase K digestion of fibrils was performed as described (17).

Far-UV CD Spectroscopy—CD spectra were acquired on a Pistar-180 spectrometer (Applied Photophysics Ltd.). Spectra were recorded between 190 and 250 nm at 25 °C in a 0.01-cm path length cuvette. Points were recorded every 1 nm at a scan rate of 20 nm/min and a bandwidth of 1 nm. Samples were prepared in Buffer A, and the buffer base line was subtracted from each spectrum. Each spectrum was the average of 10 scans and was smoothed. The CD signal is expressed as mean residue ellipticity.

Electron Microscopy—5-μl aliquots of the fibril suspension were applied to carbon-coated copper grids for 1 min. The grids were blotted, washed twice in droplets of double-distilled water, stained with 1% uranyl acetate, and observed with a Phillips Tecnai 20 electron microscope at 120 kV.

RESULTS

Assembly of Ure2p Fibrils Is Dramatically Accelerated by the Presence of a Disulfide Bond at Site 17—Cysteine scanning of amyloidogenic proteins has been used to study the structure of amyloid fibrils and to try to understand the driving force behind amyloid formation (13, 27–29). In this study, the first 70 residues within the PrD of Ure2p were each replaced in turn by cysteine, except for the Asn and Gln residues, as these residues are believed to contribute to the formation of amyloid aggregates (14, 40–43). In total, 35 cysteine substitution mutants of Ure2p were constructed (supplemental Fig. S1). Under oxidizing conditions (*i.e.* in the presence of 3 mM H_2O_2), each of these single substitution cysteine mutants inhibited fibril formation of Ure2p to varying extents (data not shown) except R17C (Fig. 1). We compared the assembly kinetics of R17C and WT under oxidizing conditions (*i.e.* 3 mM H_2O_2), partially oxidizing conditions (*i.e.* in the absence of oxidizing or reducing agents but simply exposed to air), or reducing conditions (*i.e.* in the presence of 64 mM DTT). Under oxidizing or partially oxidizing conditions, R17C displayed a much shorter lag time than WT (Fig. 1*A*). However, under reducing conditions, R17C showed a much longer lag time than WT (Fig. 1*B*). The results suggest

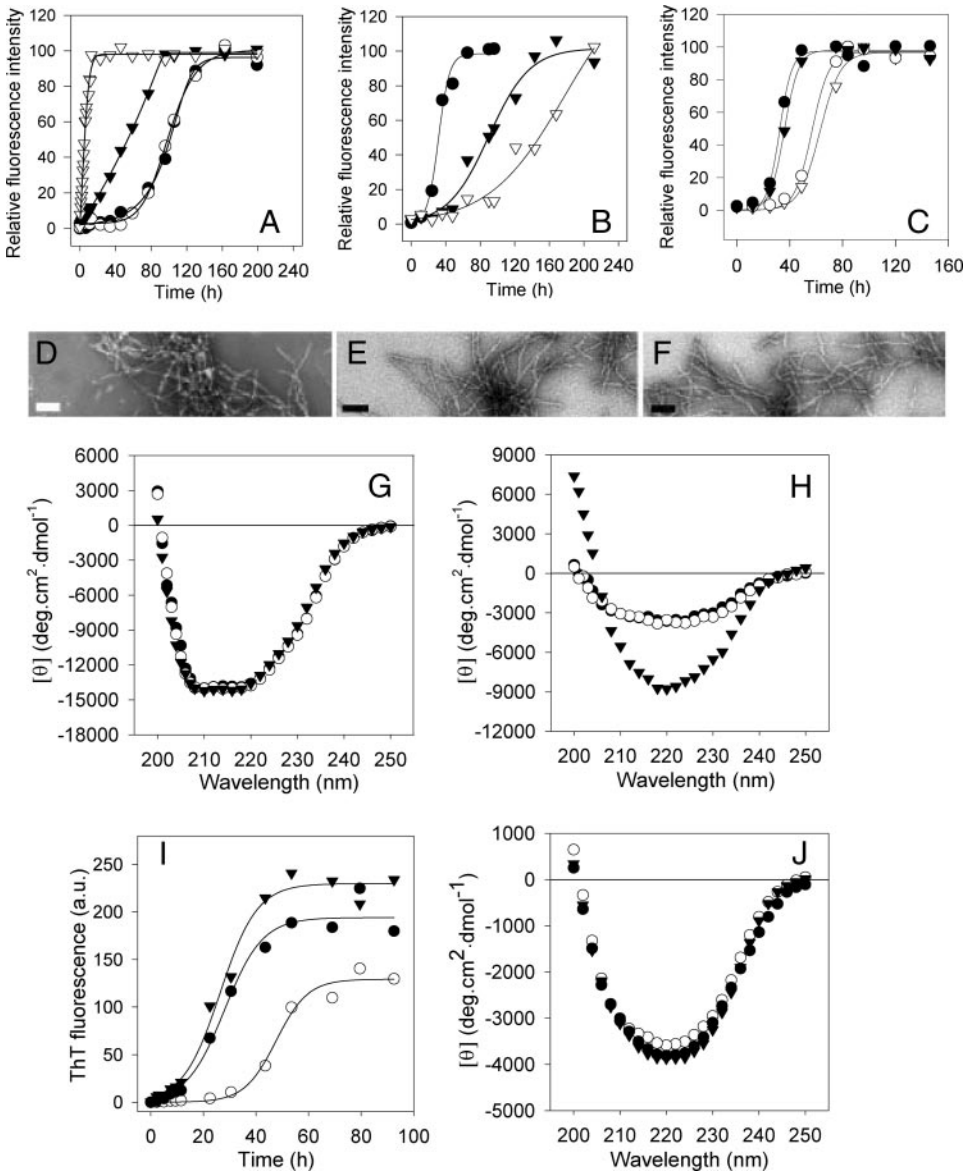

FIGURE 1. **Ure2p mutant R17C forms fibrils under oxidative conditions with morphology indistinguishable from that of WT but with faster assembly kinetics.** *A–C*, fibril formation kinetics monitored by ThT binding. Incubation was at 8 °C in Buffer A without agitation. *A*, 30 μM WT (●, ○) and R17C (▼, ▽) in the presence of 3 mM H_2O_2 (○, ▽) and in its absence (●, ▼). *B*, 30 μM WT (●), 30 μM R17C (▽), and 60 μM R17C (▼) in the presence of 64 mM DTT. *C*, 30 μM WT (●, ○) and R17S (▼, ▽) in the presence of 64 mM DTT (●, ▼) and in its absence (○, ▽). *D–F*, EM images of WT and R17C fibrils. *Scale bars* = 200 nm. *D*, R17C formed in the presence of 3 mM H_2O_2. *E*, WT formed in the presence of 3 mM H_2O_2. *F*, WT formed in the absence of oxidizing agent. *G* and *H*, far-UV CD spectra of 30 μM WT (●, ○) and R17C (▼) before (*G*) and after (*H*) fibril formation recorded at 25 °C in Buffer A with (●, ▼) and without (○) 3 mM H_2O_2. *I* and *J*, fibril formation kinetics monitored by ThT binding (*I*) and far-UV CD spectra of fibrils (*J*) for WT fibrils formed in the absence of seed (○) and in the presence of 1% (w/w) WT (●) or R17C (▼) seeds. *deg*, degrees; *a.u.*, arbitrary units.

that the presence of a disulfide bond at site 17 facilitates fibril formation for Ure2p. The thiol group of R17C was readily oxidized to form a disulfide bridge, and so high concentrations of DTT were required to prevent its formation. The same concentration of DTT was found to accelerate the assembly reaction for WT (Fig. 1*C*) for reasons that are not currently understood. The thiol group of R17C may form an adjunct with DTT, which would interfere with the fibril assembly of R17C and would explain why it forms fibrils more slowly than WT under reducing conditions. To test this possibility, R17S was constructed, and its rate of fibril assembly was compared with that of WT. The results showed that R17S and WT had very similar fibril assembly kinetics both in the presence of 64 mM DTT and in its absence (Fig. 1*C*). This suggests that the apparent difference in the fibril formation kinetics of WT and R17C under reducing conditions is due to the opposing effects of interaction with DTT on these two proteins rather than a difference in the fibril-forming propensity of reduced R17C and WT *per se*.

Electron microscopy (EM) images (Fig. 1, *D–F*) showed that the morphology of R17C fibrils was indistinguishable from that of WT fibrils, with an apparent diameter of ~25 nm, in agreement with previous results for WT Ure2p (17). We compared the enzymatic activity of WT and R17C fibrils and found they retained similar levels of activity (data not shown), ruling out any significant disturbance of the C-terminal domain structure by cross-link formation. Fibrils of WT and R17C were digested with proteinase K and imaged by EM (supplemental Fig. S2), showing very similar results to those reported previously for WT Ure2p (17), indicating a fibril core of ~4 nm for both WT and R17C. These results imply that fibrils formed from oxidized R17C have essentially the same fibril structure as WT Ure2p.

The CD spectrum of native full-length Ure2p showed two minima at ~208 and 222 nm (Fig. 1*G*), which is typical for a protein rich in α-helical content. After the assembly reaction, the CD spectrum changed to show only one minimum at ~220 nm (Fig. 1*H*), which suggests an increase in β-sheet structure. We compared the CD spectra of oxidized R17C and WT before and after fibril assembly. Although they had identical CD spectra before fibril assembly (Fig. 1*G*), R17C had a stronger CD signal after fibril assembly compared with WT (Fig. 1*H*). This presents two possibilities. One is that R17C contains more β-sheet structure within the same amount of fibrils, which would mean that the secondary structure within R17C fibrils is different from that within WT fibrils (when both types of fibrils were prepared under oxidizing conditions). The other possibility is that R17C forms more fibrils and less amorphous aggregates than WT, but its fibrils have the same secondary structure as the WT fibrils. (During the fibril

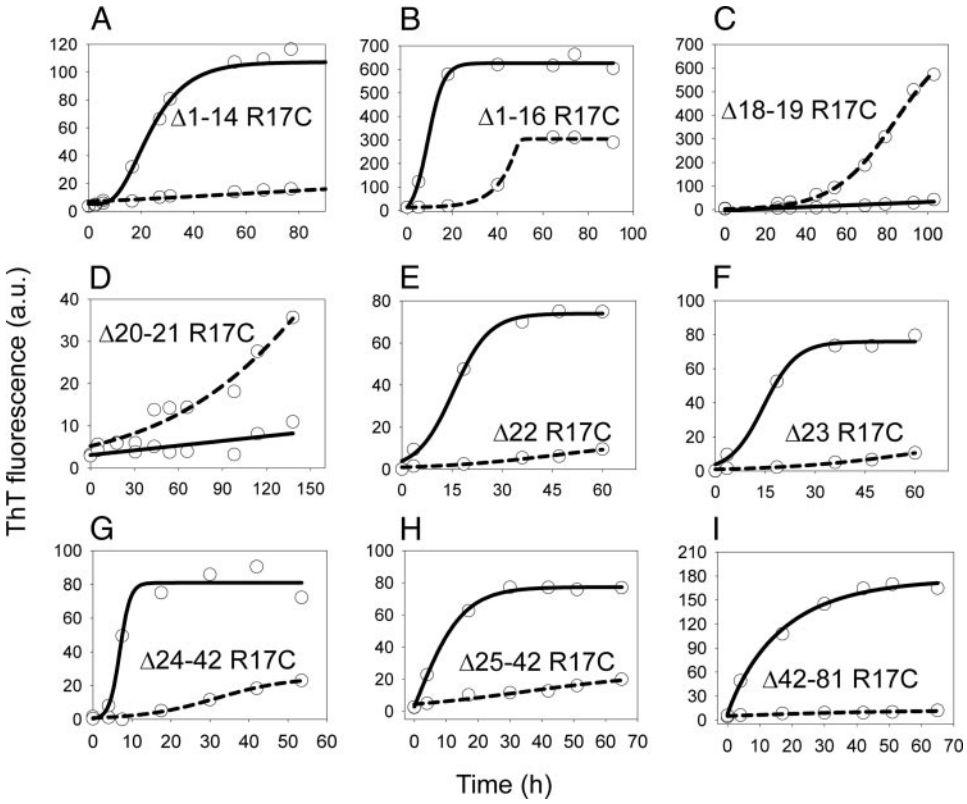

FIGURE 2. **Comparison of the assembly kinetics of deletion mutants of R17C Ure2p.** *Solid lines*, in the presence of 3 mM cumene hydroperoxide as an oxidizing agent; *dashed lines*, with 3 mM DTT as a reducing agent. The deletion mutants were as indicated. The protein concentration was 80 μM, except as indicated: 60 μM (*A*), 150 μM (*B*), 120 μM (*C*), and 100 μM (*D*). Other conditions were as described in the legend to Fig. 1 (*A–C*). *a.u.*, arbitrary units.

assembly reaction, amorphous aggregates always appear, and sometimes they co-aggregate with fibrils, so it is hard to separate fibrils and amorphous aggregates.) To distinguish between these two possibilities, we compared the seeding properties of WT and R17C using preformed fibrils prepared under oxidizing conditions. Both WT and R17C could seed WT Ure2p to form fibrils, and the kinetics were similar for the two types of seeds (Fig. 1*I*). Furthermore, the CD spectra after seeding showed that fibrils induced by R17C seeds had the same spectrum as those induced by WT seeds (Fig. 1*J*). This demonstrates that the structure of R17C fibrils assembled under oxidizing conditions is the same as that of WT fibrils. Furthermore, under oxidizing conditions, R17C is able to form fibrils more efficiently than WT, leading to reduced formation of amorphous aggregates.

The Disulfide Bond at Site 17 Accelerates the Assembly of Ure2p Fibrils by Bringing a Specific Stretch in the Two Polypeptide Chains into Proximity—To understand why, of 35 cysteine substitutions within the PrD, only a disulfide bond at site 17 can promote the kinetics of assembly significantly, we produced mutants of R17C containing deletions of neighboring sequence regions in an attempt to disrupt its ability to assemble rapidly into fibrils under oxidative conditions. When the region of Ure2p prior to site 17 was truncated, R17C retained its ability to assemble into fibrils under oxidizing conditions (Fig. 2, *A* and *B*; and supplemental Fig. S3, *A* and *B*), which suggests that the disulfide bond at site 17 has no direct effect on the region extending from residues 1 to 16. Interestingly, however, when residues 18–19 or 20–21 were deleted, the oxidized form of R17C lost its ability to form fibrils (Fig. 2, *C* and *D*; and supplemental Fig. S3, *C* and *D*). In contrast, any deletion in region 22–81 did not prevent fast assembly of oxidized R17C into fibrils (Fig. 2, *E–I*; and supplemental Fig. S3, *E–I*). Furthermore, even where the mutant tended to form only short fibrils, such as R17CΔ42–81 (supplemental Fig. S3*I*), perhaps because of disruption of the linker region formed by residues 66–90 (17), the deletion mutants of R17C were nevertheless able, like R17C, to seed fibril formation of WT Ure2p (supplemental Fig. S4). These data suggest that the specific region 18–21 plays a critical role in the ability of oxidized R17C to assemble rapidly into fibrils.

Short peptides (typically 4–7 amino acids) that can form fibrils when isolated from the intact protein have been found for Sup35, amyloid-β, IAPP, and many other amyloid-related proteins (34), but no such short peptides have previously been identified for Ure2p. We synthesized three Ure2p peptides containing the R17C mutation, CQVNIG (residues 17–22), CQVNIGN (residues 17–23), and CQVNIGNR (residues 17–24), all of which were found to form fibrils under oxidizing conditions (data not shown). The 8-residue peptide CQVNIGNR had much better solubility than the other two, so we chose this peptide for further study.

When peptide CQVNIGNR was dissolved in Buffer A, it showed a minimum at ~194 nm in the CD spectrum (Fig. 3*A*), which indicates a random coil structure. Upon the addition of H_2O_2, it underwent a conformational change within minutes, as detected by an increase in ThT binding fluorescence (Fig. 3*B*), and the presence of aggregates was apparent to the naked eye. The pellets were collected, and the CD spectrum of the aggregates was recorded, showing a single minimum at ~230 nm (Fig. 3*A*). We interpreted this peak as an indication of β-sheet structure. CD is normally used to detect protein secondary structure in the soluble state, and visible aggregates will cause light scattering, which interferes with the CD signal. We therefore sonicated the pellets gently to reduce the size of the aggregates and to cause them to be dispersed homogeneously in solution. EM images before and after sonication confirmed that the aggregates remained as fibrils after this treatment (Fig. 3, *C* and *D*). The CD spectra of the fibrils after sonication showed a shift in the single minimum to ~220 nm, the hallmark of β-sheet structure, and the magnitude of the signal also increased (Fig. 3*A*) so that the spectrum resembled that for

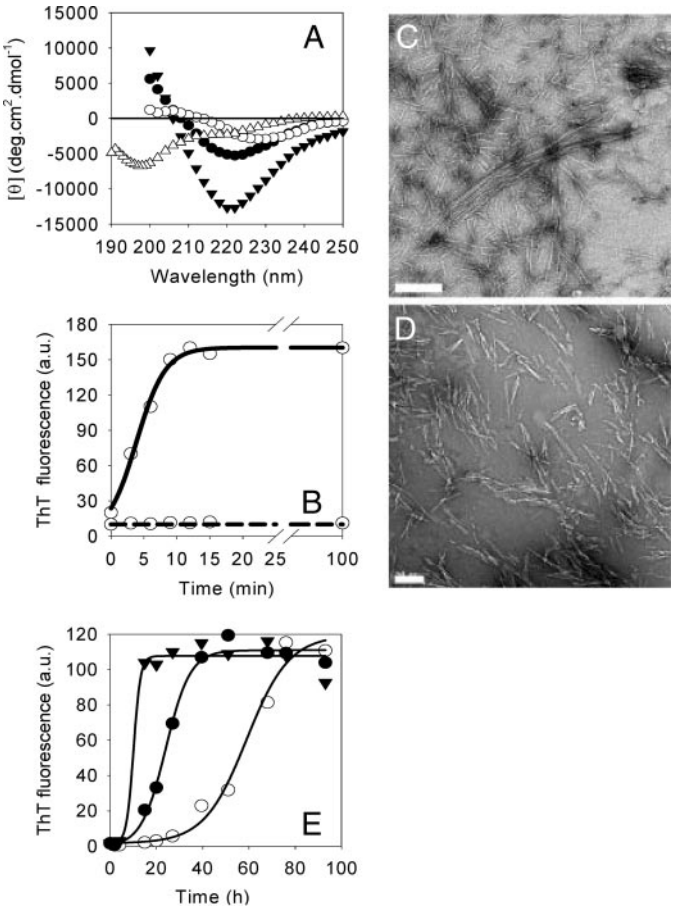

FIGURE 3. **Peptide CQVNIGNR forms fibrils under oxidizing conditions and seeds WT Ure2p.** *A*, far-UV CD spectra of peptide CQVNIGNR: soluble state in Buffer A (△), fibrils formed in the presence of 3 mM H_2O_2 (○), and fibrils after sonication for 6 s (●) or 40 s (▼). *B*, assembly kinetics of CQVNIGNR (1 mg/ml) in the presence of 3 mM H_2O_2 (*solid line*) or 3 mM DTT (*dashed line*) in Buffer A. *C* and *D*, EM images of negatively stained fibrils of CQVNIGNR formed in the presence of 3 mM H_2O_2 before (*C*) and after (*D*) sonication for 60 s. *E*, time course of seeded assembly of WT in the presence of 0% (○), 3% (●), and 15% (▼) (w/w) preformed fibrils of CQVNIGNR. *deg*, degrees; *a.u.*, arbitrary units.

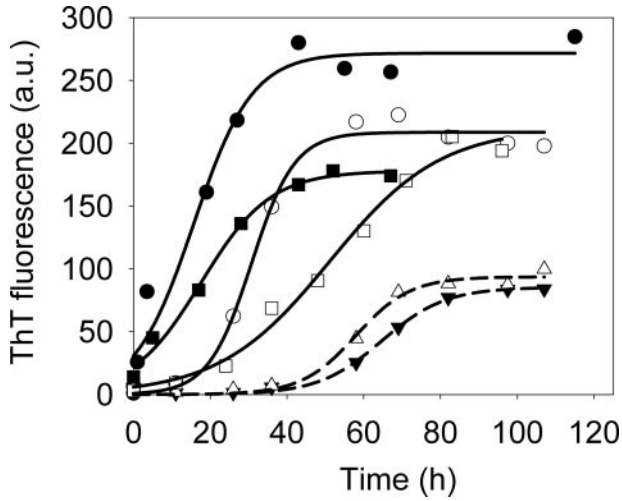

FIGURE 4. **Comparison of the assembly kinetics of different substitution mutants of Ure2p at site 17.** The protein concentration was 30 μM. Other conditions were as described in the legend to Fig. 1 (*A–C*). △, WT; ●, R17F; ■, R17L; ○, ΔR17; □, R17M; ▼, R17K. *a.u.*, arbitrary units.

fibrils of full-length WT and R17C Ure2p (Fig. 1, *H* and *J*). The fibrils formed by peptide CQVNIGNR were ~3 nm in diameter (Fig. 3, *C* and *D*), much thinner than those formed from full-length Ure2p but reminiscent of the amyloid core of protease-digested Ure2p fibrils (17). Like fibrils of full-length R17C (Fig. 1*J*), the peptide fibrils were found to seed soluble full-length WT Ure2p to form fibrils (Fig. 3*E*).

We concluded that QVNI (residues 18–21 in Ure2p) represents a potential amyloid stretch, which does not necessarily form fibrils itself but has the ability to form amyloid fibrils with the help of additional stabilizing interactions between the peptide molecules. For example, when this stretch is capped by cysteine and then oxidized, the disulfide bond will bring the two of these sequence regions close in space and provide the opportunity for interactions to form. Alternatively, the disulfide bond may confine the backbone of the stretch in a conformation that is favorable for conversion to β-sheet structure. In the case of the full-length protein, when the disulfide bridge forms at site 17, the potential stretch may undergo a rapid conformational change from random coil to β-sheet; then following this, the structure of other regions in the PrD will be converted under the direction of this potential amyloid stretch.

Hydrophobic Substitution at Site 17 Increases the Assembly Reaction of Ure2p to Varying Extents by Increasing the Assembly Properties of the Potential Amyloid Stretch—Our results suggest that site 17 plays an important role in the fibril formation process. We therefore made additional mutants to determine which types of mutation affect the assembly kinetics of Ure2p. Site 17 was deleted (ΔR17) or replaced by a hydrophobic (Val, Leu, Ile, Phe, Met) or charged (Lys) residue. The results for those mutants that could be successfully purified are shown in Fig. 4. (The result of substitution with the polar residue Ser is shown above in Fig. 1*C*.) We found that when Arg^{17} was deleted or substituted by a hydrophobic residue, the rate of fibril assembly increased to varying extents, whereas the rates of assembly for R17S and R17K were similar or slightly slower than those for WT. The presence of amyloid fibrils in each case was confirmed by EM (supplemental Fig. S5). The Ure2p mutants R17F and R17L expressed well in *E. coli*, but most of the protein was found in the cell pellet, so the final yield of purified protein was only ~1% of the amount typically obtained for WT. These mutants were purified and then, after rapid buffer exchange, directly used for experiments (see "Experimental Procedures") because the lag time for assembly into fibrils was <4 h (Fig. 4). R17V and R17I could not be obtained as soluble protein because they were found as inclusion bodies in the cell. However, their high tendency to aggregate in *E. coli* cells probably reflects a high tendency to form amyloid fibrils.

We hypothesized that the acceleration of fibril assembly for mutants of Ure2p in which Arg^{17} has been replaced by a hydrophobic residue may be caused by an increase in the fibril-forming propensity of the adjacent potential amyloid stretch (QVNI). To test this idea, we made synthetic peptides corresponding to Ure2p residues 17–24 (RQVNIGNR) and 18–24 (QVNIGNR) and also a series of *X*QVNIGNR peptides (where *X* represents Val, Phe, Met, Leu, or Ile) and allowed the peptides to form fibrils. CD spectra of the *X*QVNIGNR peptides in the soluble state showed a negative peak at ~196 nm, which sug-

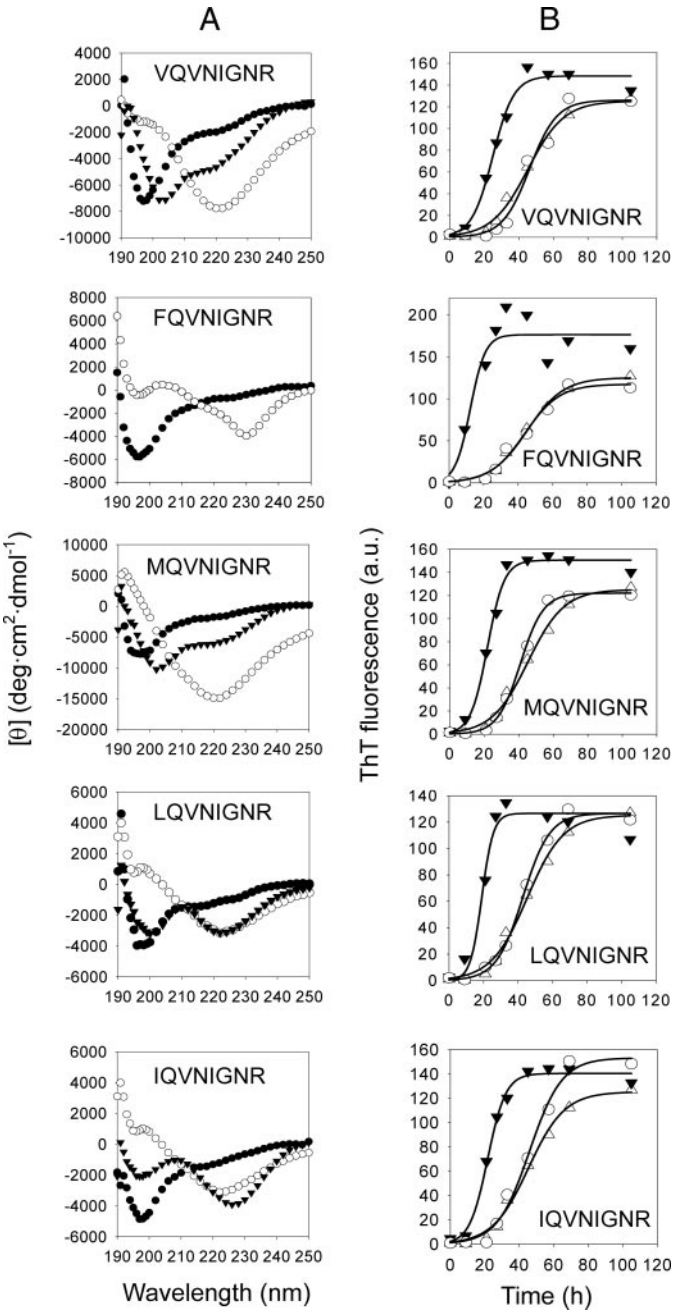

FIGURE 5. ***XQVNIGNR octapeptides (where X is a hydrophobic residue) can form fibrils that seed WT Ure2p.*** *A*, far-UV CD spectra of different *X*QVNIGNR octapeptides (where *X* represents Val, Phe, Met, Leu, or Ile) before fibril formation (●) ($t = 0$), during fibril formation (▼) ($t = 12$ h), and after fibril formation (○) ($t = 5$ days). Incubation was with shaking for 5 days at 8 °C. The peptide concentration was 2 mg/ml. (The spectrum of FQVNIGNR during fibril formation could not be obtained because of the very rapid rate of fibril assembly.) *B*, time course of fibril formation for 30 μM WT Ure2p alone (○), in the presence of 0.1 mg/ml soluble octapeptide (△), or in the presence of 0.1 mg/ml preformed fibrils made from the octapeptide (▼). *deg*, degrees; *a.u.*, arbitrary units.

gests unfolded structure, and after fibril formation, a single minimum appeared at ~220–230 nm, which indicates β-sheet content (Fig. 5*A*). We also investigated the seeding properties of these fibrils, and the results showed that, in each case, they could seed full-length Ure2p to form fibrils (Fig. 5*B*). Furthermore, these peptides were observed by EM to form thin fibrils with a diameter of 3 nm (Fig. 6).

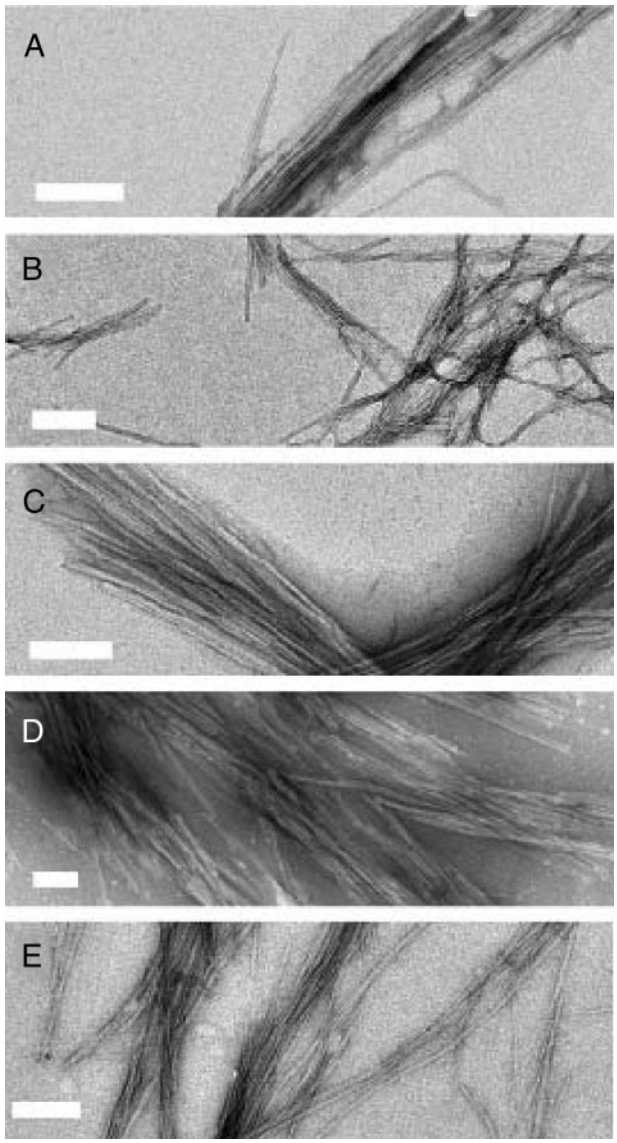

FIGURE 6. **Electron micrographs of negatively stained fibrils of *XQVNIGNR* octapeptides.** Assembly conditions were as described in the legend to Fig. 5. *Scale bars* = 200 nm. *A*, VQVNIGNR; *B*, FQVNIGNR; *C*, MQVNIGNR; *D*, LQVNIGNR; *E*, IQVNIGNR.

Whereas the *X*QVNIGNR peptides all formed fibrils within days on standing at 8 °C, under the same conditions, the WT sequence peptides QVNIGNR and RQVNIGNR did not readily form fibrils. However, after incubation at a concentration of 4 mg/ml at 8 °C for 3 months, peptide RQVNIGNR formed long straight fibrils visible by EM (supplemental Fig. S6). (The amount of fibrils was insufficient to perform further experiments). These results imply that when the potential amyloid stretch is capped by a hydrophobic residue, it can form fibrils extremely readily. Thus, in the case of the full-length protein, we can attribute the relatively fast fibril-forming ability of R17F, R17L, R17M, and ΔR17 to the increased fibril-forming propensity of the potential amyloid stretch when capped by a hydrophobic residue. When arginine is deleted from site 17, Leu[16] is then adjacent to the potential amyloid stretch, and so the presence of this hydrophobic residue allows rapid fibril formation.

DISCUSSION

In this study, we have identified a 4-residue potential amyloid stretch within Ure2p (QVNI, residues 18–21) and characterized the properties of peptides containing this sequence as well as the effect of mutations adjacent to this stretch on the fibril-forming propensity of full-length Ure2p. This region is located in the highly conserved, non-Asn/Gln repeat region of the PrD of Ure2p (44). There may be additional potential amyloid stretches in Ure2p, as has been found in other amyloid-related proteins such as Sup35 and β-microglobulin, each of which contains several amyloid stretches. If this entire region (residues 15–42) is deleted, Ure2p still retains its ability to assemble into highly ordered amyloid fibrils, although with a longer lag time, as we have shown previously (14).

There are several lines of evidence that the PrD of Ure2p adopts an in-register parallel β-sheet structure in the fibrillar state (45–47). Amyloid fibrils formed from the *X*QVNIGNR octapeptides can behave as seeds to accelerate the conformational conversion of soluble Ure2p into amyloid fibrils. Therefore, this suggests that the fibrils made from *X*QVNIGNR have the same core structure as the full-length Ure2p fibrils. In a model for the structure of fibrils formed by the Ure2p PrD (48), sequence RQVNIGNR is predicted to exist as an intact β-strand, which is compatible with the results of this study. Comparison of the amyloid-forming ability of RQVNIGNR (residues 17–24 of WT Ure2p) with that of *X*QVNIGNR suggests that hydrophobic interactions including the first position of *X*QVNIGNR help serve as a driving force for assembly of the peptides into fibrils in a self-catalytic manner. In addition, our findings show that generic hydrophobic residues, not specific amino acids, are sufficient to increase the fibril-forming propensity, although different residues show differences in the kinetics of amyloid assembly. Similar results have been found for the Aβ42 peptide (49). These results indicate that the sequence pattern of the amyloid stretch is not a strict one and that sometimes it can accept mild variation of residues with similar physicochemical properties.

The results presented above imply that single hydrophobic substitution mutants at site 17 (R17F, R17L, R17M, and ΔR17) accelerate Ure2p assembly through increasing the amyloid-forming propensity of the adjacent segment extending from residues 18 to 21 of Ure2p. This strongly supports the amyloid stretch hypothesis (36), which suggests that the driving force of protein aggregation can be confined to a small region of the intact protein.

Our present data also shed light on the strategy Ure2p has adopted to combat unwanted aggregation. Arg^{17} is located between the potential amyloid stretch and a hydrophobic residue, Leu^{16}, so it is likely that Arg^{17} functions as a gatekeeper residue that interrupts an intact amyloid stretch (LQVNI) to ensure that protein aggregation occurs at a low frequency under normal conditions and allows Ure2p to function in the negative control of nitrogen catabolism. Similar strategies are found in other proteins. It has been shown that charged residues interrupt contiguous stretches of hydrophobic residues to allow proteins to escape aggregation (50).

Previous studies have focused on how protein folding relates to protein misfolding; for example, many proteins must convert from the fully folded state to a partially folded state before aggregation initiates, and protein folding is considered as a way to escape protein misfolding or aggregation (51). It seems that the factors governing protein folding and misfolding may be totally different, perhaps working in opposition. However, in principle, protein folding, which usually involves only one polypeptide chain, and protein misfolding, which often involves multiple polypeptide chains, both involve protein conformational change. From this point of view, protein folding and misfolding should share common characteristics. Therefore, findings from protein folding should shed light on the study of protein misfolding. In the study of protein folding, hydrophobic core composition is found to be a determinant of the folding rate (52). Similarly, hydrophobicity in critical regions of a polypeptide chain has a marked effect on its aggregation propensity. Here, our results show that generic hydrophobic substitutions at site 17 can significantly accelerate the aggregation rate of Ure2p.

It has been reported that disulfide bonds contribute greatly to protein stability and folding rates (18–21). The enhancement of protein folding rate depends on the position of a disulfide bond (20). Interestingly, our data show that whereas a disulfide bond at site 17 in Ure2p significantly accelerates the aggregation rate, disulfide bonds at 41 other positions introduced by us in this study or previously by Melki and co-workers (13, 27) cause inhibition of amyloid fibril formation.

In the folding process, the sequence of events is relatively constrained; therefore, it is reasonable to predict that the disulfide bond, which can greatly accelerate the folding process, should be located in a protein region involved in the early stages of the folding process. However, upon misfolding, it is hard to precisely determine which region of the protein converts to β-sheet structure first because amyloid fibrils made from the same protein show different morphologies, which may be based on differences in the content of β-sheet structure or on differences in the manner of packing within protofibrils. Generally, if the disulfide bond is to affect the kinetics of protein misfolding, it should be located in the amyloid core region in the fibrillar state. Previous studies on fibrils by solid-state NMR (46, 47) showed that residues 17–21 in WT Ure2p are located entirely within the amyloid core region.

It has been shown that a disulfide bond accelerates the folding rate by stabilizing native-like topology (53) or can influence the relative contact order (26). In the case of misfolding, we suppose a disulfide bond provides opportunities for interactions involving the potential amyloid stretch by bringing two peptides into proximity. The disulfide bond may also act as a conformational constraint to confine the backbone of the polypeptide chain in a manner that is favorable for β-sheet conversion, allowing multiple peptide chains to come together in a conformation favorable for amyloid fibril assembly. The similarity in morphology of fibrils of WT and R17C Ure2p, both before (Fig. 1, *D–F*) and after (supplemental Fig. S2) proteinase K digestion, together with the ability of fibrils formed from both full-length R17C (Fig. 1, *G–J*) and its peptides (Fig. 3) to seed WT Ure2p, suggests that the formation of a disulfide cross-link at site 17 constrains the peptide sequence in a way that is com-

patible with the WT Ure2p fibril structure and facilitates its formation.

Acknowledgments—We thank the Center for Biological EM, Institute of Biophysics, for assistance with experiments and Dr. Xinyu Wang and Yiqian Wang for helpful discussions.

REFERENCES

1. Wickner, R. B. (1994) *Science* **264,** 566–569
2. Masison, D. C., and Wickner, R. B. (1995) *Science* **270,** 93–95
3. Thual, C., Komar, A. A., Bousset, L., Fernandez-Bellot, E., Cullin, C., and Melki, R. (1999) *J. Biol. Chem.* **274,** 13666–13674
4. Perrett, S., Freeman, S. J., Butler, P. J., and Fersht, A. R. (1999) *J. Mol. Biol.* **290,** 331–345
5. Thual, C., Bousset, L., Komar, A. A., Walter, S., Buchner, J., Cullin, C., and Melki, R. (2001) *Biochemistry* **40,** 1764–1773
6. Pierce, M. M., Baxa, U., Steven, A. C., Bax, A., and Wickner, R. B. (2005) *Biochemistry* **44,** 321–328
7. Taylor, K. L., Cheng, N., Williams, R. W., Steven, A. C., and Wickner, R. B. (1999) *Science* **283,** 1339–1343
8. Bousset, L., Belrhali, H., Janin, J., Melki, R., and Morera, S. (2001) *Structure* **9,** 39–46
9. Umland, T. C., Taylor, K. L., Rhee, S., Wickner, R. B., and Davies, D. R. (2001) *Proc. Natl. Acad. Sci. U. S. A.* **98,** 1459–1464
10. Bai, M., Zhou, J. M., and Perrett, S. (2004) *J. Biol. Chem.* **279,** 50025–50030
11. Baxa, U., Ross, P. D., Wickner, R. B., and Steven, A. C. (2004) *J. Mol. Biol.* **339,** 259–264
12. Zhang, Z. R., Bai, M., Wang, X. Y., Zhou, J. M., and Perrett, S. (2008) *J. Mol. Biol.* **384,** 641–651
13. Bousset, L., Thomson, N. H., Radford, S. E., and Melki, R. (2002) *EMBO J.* **21,** 2903–2911
14. Jiang, Y., Li, H., Zhu, L., Zhou, J. M., and Perrett, S. (2004) *J. Biol. Chem.* **279,** 3361–3369
15. Catharino, S., Buchner, J., and Walter, S. (2005) *Biol. Chem.* **386,** 633–641
16. Ranson, N., Stromer, T., Bousset, L., Melki, R., and Serpell, L. C. (2006) *Protein Sci.* **15,** 2481–2487
17. Baxa, U., Taylor, K. L., Wall, J. S., Simon, M. N., Cheng, N., Wickner, R. B., and Steven, A. C. (2003) *J. Biol. Chem.* **278,** 43717–43727
18. Matsumura, M., Signor, G., and Matthews, B. W. (1989) *Nature* **342,** 291–293
19. Clarke, J., and Fersht, A. R. (1993) *Biochemistry* **32,** 4322–4329
20. Mason, J. M., Gibbs, N., Sessions, R. B., and Clarke, A. R. (2002) *Biochemistry* **41,** 12093–12099
21. Knowles, T. P., and Zahn, R. (2006) *Biophys J.* **91,** 1494–1500
22. Creighton, T. E. (1992) *Science* **256,** 111–114
23. Creighton, T. E. (1992) *BioEssays* **14,** 195–199
24. Mason, J. M., Cliff, M. J., Sessions, R. B., and Clarke, A. R. (2005) *J. Biol. Chem.* **280,** 40494–40499
25. Feige, M. J., Hagn, F., Esser, J., Kessler, H., and Buchner, J. (2007) *J. Mol. Biol.* **365,** 1232–1244
26. Parrini, C., Bemporad, F., Baroncelli, A., Gianni, S., Travaglini-Allocatelli, C., Kohn, J. E., Ramazzotti, M., Chiti, F., and Taddei, N. (2008) *J. Mol. Biol.* **379,** 1107–1118
27. Fay, N., Redeker, V., Savistchenko, J., Dubois, S., Bousset, L., and Melki, R. (2005) *J. Biol. Chem.* **280,** 37149–37158
28. Krishnan, R., and Lindquist, S. L. (2005) *Nature* **435,** 765–772
29. Fayard, B., Fay, N., David, G., Doucet, J., and Melki, R. (2006) *J. Mol. Biol.* **356,** 843–849
30. Shivaprasad, S., and Wetzel, R. (2006) *J. Biol. Chem.* **281,** 993–1000
31. Wetzel, R., Shivaprasad, S., and Williams, A. D. (2007) *Biochemistry* **46,** 1–10
32. Tenidis, K., Waldner, M., Bernhagen, J., Fischle, W., Bergmann, M., Weber, M., Merkle, M. L., Voelter, W., Brunner, H., and Kapurniotu, A. (2000) *J. Mol. Biol.* **295,** 1055–1071
33. Ivanova, M. I., Thompson, M. J., and Eisenberg, D. (2006) *Proc. Natl. Acad. Sci. U. S. A.* **103,** 4079–4082
34. Sawaya, M. R., Sambashivan, S., Nelson, R., Ivanova, M. I., Sievers, S. A., Apostol, M. I., Thompson, M. J., Balbirnie, M., Wiltzius, J. J., McFarlane, H. T., Madsen, A. O., Riekel, C., and Eisenberg, D. (2007) *Nature* **447,** 453–457
35. Lopez de la Paz, M., and Serrano, L. (2004) *Proc. Natl. Acad. Sci. U. S. A.* **101,** 87–92
36. Esteras-Chopo, A., Serrano, L., and Lopez de la Paz, M. (2005) *Proc. Natl. Acad. Sci. U. S. A.* **102,** 16672–16677
37. Nelson, R., Sawaya, M. R., Balbirnie, M., Madsen, A. O., Riekel, C., Grothe, R., and Eisenberg, D. (2005) *Nature* **435,** 773–778
38. Miroux, B., and Walker, J. E. (1996) *J. Mol. Biol.* **260,** 289–298
39. Zhu, L., Zhang, X. J., Wang, L. Y., Zhou, J. M., and Perrett, S. (2003) *J. Mol. Biol.* **328,** 235–254
40. Perutz, M. F., Johnson, T., Suzuki, M., and Finch, J. T. (1994) *Proc. Natl. Acad. Sci. U. S. A.* **91,** 5355–5358
41. Perutz, M. F., Pope, B. J., Owen, D., Wanker, E. E., and Scherzinger, E. (2002) *Proc. Natl. Acad. Sci. U. S. A.* **99,** 5596–5600
42. Perutz, M. F., and Windle, A. H. (2001) *Nature* **412,** 143–144
43. Thakur, A. K., and Wetzel, R. (2002) *Proc. Natl. Acad. Sci. U. S. A.* **99,** 17014–17019
44. Edskes, H. K., and Wickner, R. B. (2002) *Proc. Natl. Acad. Sci. U. S. A.* **99,** 16384–16391
45. Ross, E. D., Baxa, U., and Wickner, R. B. (2004) *Mol. Cell. Biol.* **24,** 7206–7213
46. Chan, J. C., Oyler, N. A., Yau, W. M., and Tycko, R. (2005) *Biochemistry* **44,** 10669–10680
47. Baxa, U., Wickner, R. B., Steven, A. C., Anderson, D. E., Marekov, L. N., Yau, W. M., and Tycko, R. (2007) *Biochemistry* **46,** 13149–13162
48. Kajava, A. V., Baxa, U., Wickner, R. B., and Steven, A. C. (2004) *Proc. Natl. Acad. Sci. U. S. A.* **101,** 7885–7890
49. Kim, W., and Hecht, M. H. (2006) *Proc. Natl. Acad. Sci. U. S. A.* **103,** 15824–15829
50. Otzen, D. E., Kristensen, O., and Oliveberg, M. (2000) *Proc. Natl. Acad. Sci. U. S. A.* **97,** 9907–9912
51. Monsellier, E., and Chiti, F. (2007) *EMBO Rep.* **8,** 737–742
52. Northey, J. G., Di Nardo, A. A., and Davidson, A. R. (2002) *Nat. Struct. Biol.* **9,** 126–130
53. Strausberg, S., Alexander, P., Wang, L., Gallagher, T., Gilliland, G., and Bryan, P. (1993) *Biochemistry* **32,** 10371–10377